JOURNAL OF AGRICULTURAL AND FOOD CHEMISTRY

Shining Light on the Differences in Molecular Structural Chemical Makeup and the Cause of Distinct Degradation Behavior between Malting- and Feed-Type Barley Using Synchrotron FTIR Microspectroscopy: A Novel Approach

PEIQIANG YU,* KEVIN DOIRON, AND DASEN LIU†

College of Agriculture and Bioresources, University of Saskatchewan, 51 Campus Drive, Saskatoon, SK, Canada, S7N 5A8

The objective of this study was to use advanced synchrotron-sourced FTIR microspectroscopy (SFTIRM) as a novel approach to identify the differences in protein and carbohydrate molecular structure (chemical makeup) between these two varieties of barley and illustrate the exact causes for their significantly different degradation kinetics. Items assessed included (1) molecular structural differences in protein amide I to amide II intensities and their ratio within cellular dimensions, (2) molecular structural differences in protein secondary structure profile and their ratios, and (3) molecular structural differences in carbohydrate component peak profile. Our hypothesis was that molecular structure (chemical makeup) affects barley quality, fermentation, and degradation behavior in both humans and animals. Using SFTIRM, the protein and carbohydrate molecular structural chemical makeup of barley was revealed and identified. The protein molecular structural chemical makeup differed significantly between the two varieties of barleys. No difference in carbohydrate molecular structural chemical makeup was detected. Harrington was lower than Valier in protein amide I, amide II, and protein amide I to amide II ratio, while Harrington was relatively higher in model-fitted protein α-helix and β-sheet, but lower in the others (β-turn and random coil). These results indicated that it is the molecular structure of protein (chemical makeup) that may play a major role in the different degradation kinetics between the two varieties of barleys (not the molecular structure of carbohydrate). It is believed that use of the advanced synchrotron technology will make a significant step and an important contribution to research in examining the molecular structure (chemical makeup) of plant, feed, and seeds.

KEYWORDS: Synchrotron; molecular structure; degradation; protein structure; carbohydrate conformation

INTRODUCTION

Conventional "wet" chemical analysis fails to reveal the inherent structure of barley and fails to link barley molecular structural information to chemical information (*1*). Conventional wet chemical analysis looks for a specific component through homogenization of the feed sample and separation of the component of interest from the complex matrix. As a result, the object of the analysis is destroyed and the information about the spatial origin and distribution of the component of interest is lost (*1*). Recently, synchrotron-based FTIR microspectroscopy (SFTIRM) has been developed as a rapid, direct, noninvasive, nondestructive, and bioanalytical technique (*2–6*). SFTIRM, taking advantage of synchrotron light brightness (100–1000 million times brighter than sunlight) and small effective source size, is capable of exploring the molecular chemistry within microstructures of biological tissues without destroying inherent structures within cellular dimension (*2, 4, 5, 7, 8*). This technique can provide four kinds of information simultaneously: tissue composition, tissue structure, tissue chemistry, and tissue environment. To date, there has been very little application of this novel synchrotron-base analytical technique to study the inherent molecular structure of plant/feed/seed in relation to feed/seed quality and fermentation behavior. In a preliminary study (*9*), we used this novel technique to study the protein to starch ratio of starch granules from endosperm and detected different ratios between the two barley samples that may be responsible for the different rumen degradation characteristics. However, differences in the protein to starch ratio were not directly proportional to rumen degradation characteristics (A. Walker and J. J. McKinnon, personal contact). These ratios made

* To whom correspondence should be addressed. Tel: +1 306 966 4132. E-mail: peiqiang.yu@usask.ca.

† Visiting professor from College of Animal Science and Technology Northeast Agricultural University, China.

10.1021/jf800015x CCC: $40.75
Published on Web 04/15/2008

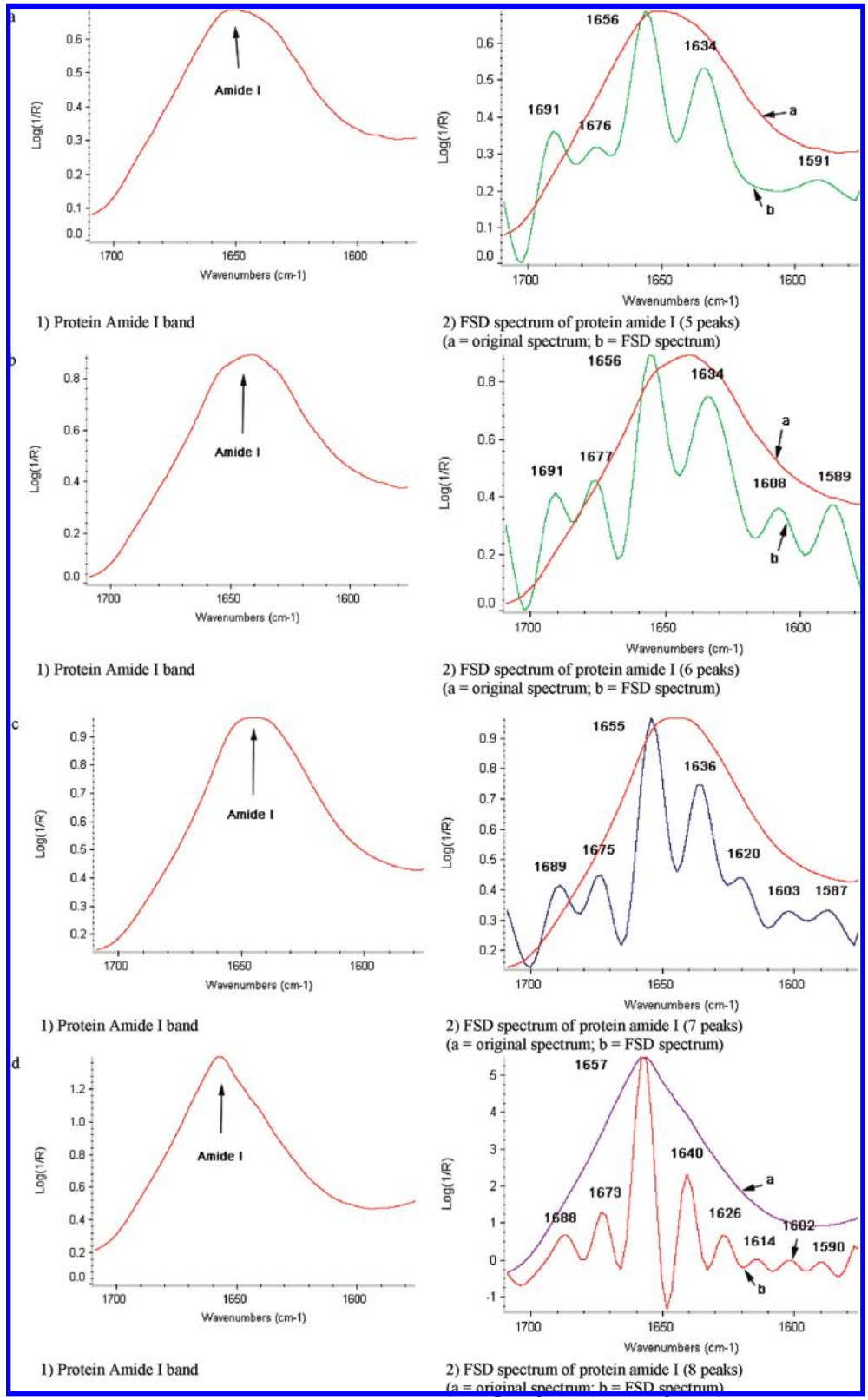

Figure 1. Typical synchrotron FTIR spectrum and Fourier self-deconvolution (FSD) spectrum of cereal grain seed tissues at a cellular level (pixel size 10 μm $\times$ 10 μm): (**a**) FSD spectrum of protein amide I with five multicomponent peaks, (**b**) FSD spectrum of protein amide I with six multicomponent peaks, (**c**) FSD spectrum of protein amide I with seven multicomponent peaks, and (**d**) FSD spectrum of protein amide I with eight multicomponent peaks.

us examine the root causes for the difference in degradation kinetics and behavior.

The objectives of this study were to use SFTIRM to reveal and identify differences in protein and carbohydrate molecular structural chemical makeup between Harrington and Valier barley. The items we assessed included (1) molecular structural differences in protein amide I to amide II intensity and ratio within cellular dimensions; (2) molecular structural differences in the secondary structure profile of protein, percentage, and their ratios of model-fitted protein α-helix, β-sheet, and others

(β-turn and random coil); and molecular structural differences in carbohydrate component peak ratio profile.

Information from this study should have value as a guide for barley breeders and for crop and feed industries to maintain and improve the nutritive value and quality of barley for both animal and human use.

The second objective of this research was to illustrate the advanced synchrotron-based analysis as a novel research tool for rapid characterization of a feed's inherent structure and molecular chemical makeup at the cellular level and to relate the inherent structural chemical makeup of a feed/seed to its nutritive value and digestive behavior.

MATERIALS AND METHODS

Barley Varieties and Synchrotron FTIR Window Preparation. Valier (MTLB-30) (a two-rowed, white kernelled, midseason spring barley) and Harrington barley (BI-704) (a two-rowed, broad and diamond-shaped kernel barley bred for malting characteristics with an extremely rapid rate of fermentation) were grown in the university research plot near Saskatoon, Canada, in 1999 and 2000, respectively. The barley samples (2 kg of each) were supplied by B. Rossnagel, Crop Development Center (CDC), the University of Saskatchewan (Saskatoon, Canada). For the in situ animal trial, around 500 g of barley seeds were randomly selected. For the synchrotron experiments, the barley seed samples were randomly selected and set on the objective disks in a microtome (Tissue Tech) and then were cut into thin cross sections (ca. 6 μm thickness) using a microtome at Western College of Veterinary, University of Saskatchewan, Saskatoon, Canada. The cross-sections of the plant tissues rapidly transferred to BaF2 windows (size 13 × 1 mm disk; part number 915-3015, Spectral Systems) for a transmission mode in synchrotron FTIR microspectroscopic work. Several cross-sections were mounted on each BaF_2 window.

Synchrotron Light Source and Fourier Transform Infrared Microspectroscopy. These experiments were performed at the National Synchrotron Light Source in Brookhaven National Laboratory (NSLS-BNL, U.S. Department of Energy). The beamlines U2B and U10B were equipped with FTIR spectrometers (ThermoNicolet, Madison, WI) with a KBr beamsplitter and liquid nitrogen cooled MCT detectors coupled with Continuμm IR microscopes with Schwartzshild 32× objective and 10× condenser. Synchrotron radiation from the VUV storage ring at the beamlines (with an energy level 800 MeV) entered the interferometer via a port of the instrument designed to detect infrared emission. The infrared spectra were collected in the mid-IR range 4000–800 cm^{-1} at a resolution of 4 cm^{-1} with 64 scans coadded in a transmission mode. The aperture setting was 10 × 10 μm. Stage control, spectrum data collection, and processing were performed using OMNIC 6.0 (Spectra Tech). Scanned visible images were obtained using a charge-coupled device (CCD) camera linked to the infrared images.

Synchrotron Data Analysis. Spectral data were collected, corrected with the background spectrum, displayed, and analyzed using OMNIC 6.0 (Spectra Tech). The data were displayed either as a series of spectroscopic images collected at individual wavelengths or as a collection of infrared spectra obtained at each pixel position in the image. Chemical functional groups (protein amide I and II, carbohydrate, protein secondary structures) were identified according to published reports (*2, 4, 5, 7, 10–12*).

Quantifying Model-Fitted α-Helix and β-Sheet in Protein Structures. A specific multipeak fitting or modeling procedure was required, because protein amide I component bands overlapped (**Figure 1**). To estimate the relative amount of model-fitted α-helix and β-sheet of the protein inherent structures, two steps were applied. The detailed procedure and comparison of Gaussian and Lorentzian methods was published in Yu (*13*). Briefly, the first step used Fourier self-deconvolution (FSD) in OMNIC to obtain the FSD spectrum in the protein amide I region at ca. 1710–1576 cm^{-1} only to identify protein amide I component peak frequencies. The detailed concepts and algorithm of FSD (a method for resolving intrinsically overlapped bands) were described by Kauppinen et al. (*14*) and Griffths and Pariente (*15*). The second step was to use a multipeak fitting program with Gaussian and Lorentzian functions using Origin data analysis software (Origin V. 6.1, OriginLab Corp., Northhampton, MA) to relatively quantify the multicomponent peak areas in protein amide I bands at ca. 1710–1576 cm^{-1} in this study. The detailed descriptions were reported in Origin in terms of peak shape, center, offset, width, and areas. The relative amount of α-helix, β-sheet, and other structures based on modeled peak areas was calculated according to the report generated by the software (*6*).

Biological Difference Determination Using an in Situ Rumen Incubation Technique. The difference between the two varieties of barley for in situ ruminal degradation was determined using the departmental standard in situ method in the fistulated dairy cattle at animal experimental station at the University of Saskatchewan. Incubation of all treatments in the rumen was with 7 g of dry matter (DM) in each coded nylon bag with the pore size of approximately 40 μm. The rumen incubations were performed according to the "gradual addition/all out" schedule. Samples were incubated in the rumen for 0, 2, 4, 8, 12, and 24 h. After incubation, the bags were removed from rumen and rinsed under a stream of cold tap water to remove excess ruminal contents and to stop microbial activity. The bags were washed with cool water without detergent and subsequently dried at 55 °C for 48 h. Dried samples were stored in a refrigerated room (4 °C) until analyzed.

In Situ Rumen Degradation Kinetics and Characteristics. Rumen degradation kinetics and characteristic of barley components [DM, crude protein (CP), and starch (ST)] were calculated using the NLIN (nonlinear) procedure of the statistical package SAS (2003) using iterative least-squares regression (Gauss–Newton method) by the following the first-order degradation kinetics equations: $R(t) = U + D \exp[-K_d(t - T_0)]$ for DM and CP, and $R(t) = D \exp(-K_d t)$ for starch (*16, 17*), where $R(t)$ stands for residue of the incubated material after t hours of rumen incubation (g/kg); U and D stand for undegraded and potentially degraded fractions, respectively (in g/kg); T_0 stands for lag time in hours; and K_d stands for degradation rate in inverse hours.

The effective degradability (ED) values were calculated as EDCP (or EDDM or EDST) (g/kg) $= S + DK_d/(K_p + K_d)$, EDCP (g/kg DM) = CP (g/kg DM) × EDCP (g/kg), EDDM (g/kg DM) = DM (g/kg DM) × EDDM (g/kg), or EDST (g/kg DM) = ST (g/kg DM) × EDST (g/kg), where the soluble fraction (S) is in g/kg. A passage rate (K_p) of 0.06/h was employed (*17*).

Rumen undegraded feed protein (RUP) and dry matter (RUDM) values were calculated as RUP (or RUDM) (g/kg) $= U + DK_p/(K_p + K_d)$, RUP (g/kg DM) = 1.11 × CP (g/kg DM) × RUP (g/kg), or RUDM = 1.11 × DM (g/kg) × RUDM (g/kg), where a K_p of 0.06/h was employed. The factor 1.11 in the formula was taken from the PDI-system and DVE/OEB system (two feed formulation models) and is the regression coefficient of ruminal in vivo on in sacco degradation data (*17*).

The rumen undegraded feed starch (RUST) values were calculated as RUST (g/kg) $= DK_p/(K_p + K_d) + 0.1S$, RUST (g/kg DM) = ST (g/kg DM) × RUST (g/kg), where a K_p of 0.06 /h was adopted (*17*). For the factor 0.1 in the formula, it was assumed that, for starch, 100 g/kg of starch in the soluble fraction (S) escapes rumen fermentation (*17*).

Statistical Analysis. Statistical analyses were performed using Proc Mixed of SAS (*18*). The Fisher's protected LSD test was used to determine differences between the barley varieties. Significance was declared at $P < 0.05$.

Multivariate Statistical Analysis for Synchrotron-Based FTIR Spectra. Multivariate analysis, principal component analysis (PCA), and hierarchical cluster analysis (CLA) were performed using Statistica software 6.0 (StatSoft Inc., Tulsa, OK) to classify and distinguish between the inherent structures of barley at a cellular level.

Cluster Analysis. The first multivariate analysis was cluster analysis of which function performs an (agglomerative hierarchical) cluster analysis of an IR spectra data set and displays the results as dendrograms. First, it calculates a distance matrix, which contains information on the similarity of spectra. Then, in hierarchical clustering, the algorithm searches within the distance matrix for the two most similar IR spectra (minimal distance). These spectra are combined into a new object (called a "cluster" or called "hierarchical group"). The

Table 1. Chemical Composition, Rumen Degradation Characteristics, and Predicted Nutrient Availability of the Malting-Type (Harrington) and Feed-Type (Valier) Barley[a]

items	barley variety	
	malting-type	feed-type
Chemical Composition		
DM (g/kg)	903	908
ash (g/kg DM)	25	22
CFat (g/kg DM)	26	27
CP (g/kg DM)	130	136
ADF (g/kg DM)	73	69
NDF (g/kg DM)	256	252
SCP (g/kg CP)	180	176
NPN (g/kg SCP)	415	354
NDICP (g/kg CP)	305	281
ADICP (g/kg CP)	38	20
In Situ Rumen Degradation Characteristics of Dry Matter		
K_d (h^{-1})	0.192	0.104
T_0 (h)	0.0	0.1
RUDM (g/kg)	370 b	528 a
EDDM (g/kg)	631 a	472 b
In Situ Rumen Degradation Characteristics of Crude Protein		
RUP (g/kg)	383 b	541 a
RUP (g/kg DM)	55 b	81 a
EDCP (g/kg)	617 a	459 b
EDCP (g/kg DM)	81 a	62 b
In Situ Rumen Degradation Characteristics of Starch		
K_d (/h)	0.065	0.026
RUST (g/kg)	342	421
RUST (g/kg DM)	153	187
EDST (g/kg)	659	579
EDST (g/kg DM)	295	256
Predicted Protein Supply and Availability Using DVE/OEB dairy System and NRC Dairy		
FOM	555 a	364 b
OEB (g/kg DM)	−34 a	−51 b
MP (g/kg DM)	95 b	107 a

[a] Means with the same letter in the same column are not significantly different.

spectral distances between all remaining spectra and the new cluster are recalculated (*19*). This technique clusters IR spectra based on similarity with other spectra.

Principal Component Analysis. The second multivariate analysis was PCA analysis, which is a statistical data reduction method. It transforms the original set of variables to a new set of uncorrelated variables called principal components (PCs). The first few PCs typically will account for >95% variance. The purpose of PCA analysis is to derive a small number of independent linear combinations (PCs) from a large set of variables that will retain as much of the information in the original variables as possible. This analysis allows the global study of the relationships between p quantitative characters (e.g., chemical functional groups) observed on n samples (e.g. FTIR spectra of feed/seed structures). The basic idea is to extract, in a multiple variable system, one, two, or sometimes more PCs that carry most of the information. These components are independent (orthogonal) of each other, and the first factor generally represents maximum variance. As factors are extracted, they account for less and less variability, and the decision of when to stop adding PCs basically depends on the point where little significant variability, or merely random noise remains. Thus, reduction of data provides a new coordinate system where axes (eigenvectors) represent the characteristic structure information of the data. Spectra then may be simply described as a function of specific properties, and not a function of intensities. The outcome of such an analysis can be presented either as 2D (two PCs) or 3D (three PCs) scatter plots (*20*).

RESULTS AND DISCUSSION

NRC Chemical Approach with Traditional "Wet" Analysis Fails To Detect Feed Intrinsic Structures and Biological Differences between Harrington and Valier Barley. The molecular structural chemical makeup of barley affects its quality, fermentation, and degradation behavior. Publications show that although Harrington barley has the same chemical composition as Valier barley, biological differences exist between the two barleys in terms of the degradation kinetics, fermentation behavior, and nutrient availability. Harrington is a malting-type barley. As with most barley varieties, its extent and rate of biodegradation in the rumen are very high. However, if ruminants consume rapidly degraded barley, the incidence of digestive disorders such as bloat and acidosis can increase. This reduces animal performance and in acute cases can lead to death (*21, 22*). Valier barley was developed recently as a specialized feed barley for ruminants (*23, 24*). Its extent and rate of rumen degradation are lower; this may prove beneficial to animal performance and health.

Availability and fermentation behavior of starch from barley are closely related to not only total chemical composition but also to the barley molecular structural chemical makeup (*25*). By conventional wet chemical analysis, we determined total chemical composition, and total chemical composition in turn is used to predict feed or seed nutritive and energy values. For example, the NRC dairy and beef requirement methods (*26, 27*) use a chemical approach to determine total feed chemical composition of most components (such as crude protein, amino acids, organic matter, ether extract) and physiochemical extraction to estimate acid detergent fiber, neutral detergent fiber, acid detergent insoluble nitrogen, and neutral detergent insoluble nitrogen. These basic chemical components are put into the NRC formula to estimate energy values for the feed [such as total digestible nutrients (TDN), total digestible neutral detergent fiber (tdNDF), total digestible crude protein (tdCP), total digestible fatty acid (tfFA), and total digestible nonfiber carbohydrate (tdNFC)], which in turn predict energy value [such as digestible energy (DE), metabolizable energy (ME), net energy (NE)] (*27*). However, the NRC chemical approach (*27*) does not accurately predict feed nutritive and energy value for many feeds. This is partly because the NRC chemical approach considers only total feed chemical and some physical components but does not consider intrinsic structure and structural chemical makeup of a feed, which are also factors associated with nutritive value.

Table 1 shows chemical composition, rumen degradation kinetics and characteristics, and predicted nutrient supply and availability of Harrington and Valier barley. The results show that differences in total chemical composition between the two varieties of barley (such as DM, CP, ADF, NDF, ADIN, NDIN) are minor. On the basis of the NRC chemical approach (*26, 27*) to predict nutritive value of these two barleys, they should have the same total nutritive and energy values. But actually they do not. From the in situ animal trial, these two barley varieties differed in rumen degradation kinetics (S, D, K_d, T_0, or ED) and effective degradation (EDDM, 631 vs 472 g/kg; EDCP, 617 vs 459 g/kg DM). From the results of modeling nutrient supply, significant differences were detected between these two barleys in both ruminal and postruminal nutrient supply [such as degraded protein balance (OEB value), −34 vs − 51 g/kg DM; total metabolized protein (MP), 95 vs 107 g/kg DM] (*17, 27*).

These results illustrate that the NRC chemical approach with the conventional wet chemical analysis failed to detect the differences between the Harrington and Valier in the in situ animal trial and failed to detect that the rumen degradation

Table 2. Intrinsic Structural Characteristics of Protein Amide I and II and Their Ratios, Revealed Using Synchrotron-Based FTIR Microspectroscopy: Comparison of Harrington (malting-type) and Valier (feed-type) Barley

items	sample number	amide profile based on the protein amide I and II peak area[a] protein amide I (~1650 cm^{-1}) (±SD[b])	protein amide II (~1550 cm^{-1}) (±SD)	ratio of protein amide I to amide II (±SD)
barley varieties				
Harrington	14	52.7 (±12.8) b	19.0 (±4.1) b	2.8 (±0.3) b
Valier	18	71.5 (±10.7) a	23.7 (±3.4) a	3.0 (±0.2) a
SEM[c]		2.93	0.934	0.06
statistics (*P* value)				
feed		<0.0001	0.0013	0.0129
barley varieties				
Harrington	14	0.7 (±0.2) b	0.3 (±0.1) b	2.3 (±0.2) b
Valier	18	1.2 (±0.3) a	0.4 (±0.1) a	2.9 (±0.3) a
SEM		0.06	0.02	0.07
statistics (*P* value)				
feed		<0.0001	<0.0001	<0.0001

[a] The protein amide data unit, IR absorbance unit. Protein peak baseline, 1718−1413 cm^{-1}; protein amide I area region, 1718−1577 cm^{-1}; protein amide II area region, 1577−1413 cm^{-1}. [b] SD = standard deviation of mean. [c] SEM = pooled standard error of means; means with the same letter in the same column are not significantly different ($P > 0.05$) by Fisher's protected LSD Method.

kinetics and effective degradability values were consistedly higher for Harrington than for Valier.

Failure of the NRC chemical approach (the wet analysis) to detect such biological differences may be because, during chemical analysis, inherent structures, biological component matrix, and potential biobarriers associated with digestive behaviors in ruminants are destroyed. A new analytical technique is needed to detect or identify differences in molecular structural chemical makeup). The synchrotron-based analytical technique may provide such information.

Protein Molecular Structural Chemical Makeup of the Two Barley Varieties. *Structural Differences in Protein Amide I to Amide II Ratio between the Two Barleys.* Each biological component in plant, seed, or feed tissue has a unique molecular chemical−structural feature; therefore, each has its own unique IR spectrum. The protein IR spectrum has two primary features, the protein amide I (ca. 1600–1700 cm^{-1}) and amide II (ca. 1500–1560 cm^{-1}) bands. These arise from specific stretching and bending vibrations of the protein backbone. The amide I band arises predominantly from the *C*═O stretching vibration (80%) of the amide *C*═O group plus the C−N stretching vibration. The amide II arises predominantly from the N−H bending vibration (60%) coupled to the C−N stretching (40%) (*12*).

The amide I and II profile depends on the protein molecular structural chemical makeup and may be affected by the processing method and variety. Recent medical research shows that, compared with normal tissue, diseased tissues (such as prion tissue) show a change in percentage of protein secondary structures and/or a reduced ratio of amide I to amide II (*4, 28, 29*).

In plant/seed/feed research, to date, no results have been published on the relationship of the amide I and amide II profiles and their ratios to nutritive value. **Table 2** shows the intrinsic structural characteristics of protein amide I and II and their ratios, revealed using the synchrotron SFTIRM. Compared to the Valier, Harrington had a significantly different amide profile ($P < 0.05$). Harrington was lower in amide I (52.7 vs 71.5, $P < 0.05$), amide II (19.0 vs 23.7, $P < 0.05$), and in the amide I to amide II ratio (2.8 vs 3.0; $P < 0.05$). These results indicated that these two barley varieties differ in protein molecular structural chemical makeup. The difference in the amide I to amide II profiles and their ratio may cause a difference in degradation between these two barley varieties.

Table 3. Characteristics of Protein Secondary Structure in Terms of the Relative Percentage of Model-Fitted α-Helix and β-Sheet of Barley Seed Estimated from Protein Amide I Region, Revealed with Synchrotron-Based FTIR Microspectroscopy and a Multipeaking Modeling Procedure: Comparison of Harrington (malting-type) and Valier (feed-type) Barley[b]

items	sample number	% of model-fitted protein secondary structures[a] α-helix (±SD[b,c])	β-sheet (±SD)[d]	others (±SD)
barley varieties				
Harrington	24	25 (±10) a	17 (±4) a	58 (±10) b
Valier	22	18 (±11) b	14 (±6) b	69 (±13) a
SEM[e]		2.1	1.0	2.4
statistics (*P* value)				
feed		0.0184	0.0248	0.0024

[a] The protein amide data unit, IR absorbance unit. [b] amide I component peak position ~ 1650 cm^{-1}. [c] SD = standard deviation of mean. [d] amide I component peak position ~ 1630 cm^{-1}. [e] SEM = pooled standard error of means; means with the same letter in the same column are not significantly different ($P > 0.05$) by Fisher's protected LSD Method.

Table 4. Characteristics of Protein Secondary Structure in Terms of α-Helix to β-Sheet Ratio of Barley Seed Estimated from the Protein Amide I Region, Revealed with Synchrotron-Based FTIR Microspectroscopy and a Multipeaking Modeling Procedure: Comparison of Harrington (Malting-Type) and Valier (Feed-Type) Barley

items	sample number	ratios of protein secondary structure[a] model-fitted α-helix to β-sheet (±SD[b])	model-fitted β-sheet to α-helix (±SD)	model-fitted α-helix to others (±SD)	model-fitted β-sheet to others (±SD)
barley varieties					
Harrington	24	1.6 (±1.0)	0.8 (±0.5)	0.5 (±0.3) a	0.3 (±0.1) a
Valier	22	1.4 (±0.9)	1.0 (±0.5)	0.3 (±0.3) b	0.2 (±0.1) b
SEM[c]		0.21	0.10	0.05	0.02
statistics (*P* value)					
feed		0.4077	0.2519	0.0248	0.0132

[a] The protein amide data unit, IR absorbance unit. [b] SD = standard deviation of mean. [c] SEM = pooled standard error of means; means with the same letter in the same column are not significantly different ($P > 0.05$) by Fisher's protected LSD method.

Differences in Protein Secondary Structure Profile, Percentage, and α-Helix to β-Sheet Ratio. The vibrational frequency of the amide I band is particularly sensitive to protein secondary structure (*4, 8, 10, 30, 31*), this can be used to determine the secondary structure of proteins. For the α-helix, the amide I typically is in the range of ca. 1648–1658 cm^{-1}. For β-sheet, the peak falls within the range of 1620–1640 cm^{-1} (*30*). The amide II [predominantly an N−H bending vibration (60%) coupled to C−N stretching (40%)] also can be used to assess protein conformation and protein molecular chemical makeup. However, it arises from complex vibrations involving multiple functional groups, so it is less useful for protein structure prediction than the protein amide I band (*12*).

The spectrum of the protein amide I original band shows a peak center at ca. 1650 and 1630 cm^{-1}. This was confirmed from the FSD spectrum of amide I at the region of 1710–1576 cm^{-1}. The protein amide I region at ca. 1710–1576 cm^{-1} was

used for multicomponent peak modeling because peaks from ca. 1576 to 1560 cm^{-1} region are not strictly amide I peaks but could be influenced by other components.

Because protein amide I component peaks overlay each other, Fourier self-deconvolution was used to obtain FSD spectra (1710–1576 cm^{-1} region) to identify amide I component peak frequencies, and then multicomponent peak fitting using Gaussian and Lorentzian functions was used to quantify the multicomponent peak area in the protein amide I region at ca. 1710–1578 cm^{-1}.

The results (**Table 3**) show that the two barleys significantly differed ($P < 0.05$) in the relative model-fitted α-helix, β-sheet, and other (β-turn and random coil) secondary structures. On the basis of multicomponent peak modeling of the protein amide I region of 1710–1576 cm^{-1}, relative to Valier, Harrington barley had relatively more model-fitted α-helix (25 vs 18%, $P < 0.05$) and β-sheet (17 vs 14%, $P < 0.05$), but relatively less of the other protein secondary structures (58 vs 69%, $P < 0.05$).

Table 4 shows the ratios of barley protein secondary structure profile. No significant differences in the α-helix to β-sheet ratio (with average ratio of 1.5, $P > 0.05$) were detected. However, significant differences in the ratios of α-helix to the other protein secondary structures (0.47 vs 0.30, $P < 0.05$) and β-sheet to the other protein secondary structures (0.31 vs 0.22, $P < 0.05$) were detected. No published results have been found for characteristics of protein secondary structures in different barley varieties, so no comparison could be made.

These results indicates that these barley varieties differed in protein secondary structure conformation in terms of percentage and ratio of protein α-helix, β-sheet, etc., indicating that they differed in protein molecular structural chemical makeup and features. These structural differences may impact barley protein utilization and availability. Our results demonstrate that ultraspatially resolved synchrotron-based analytical technique used to localize relatively pure protein bodies may reveal differences in protein molecular structural chemical makeup at a cellular level that may predict barley fermentation characteristics and nutritive values. The different protein α-helix and β-sheet structures, by altering access to gastrointestinal digestive enzymes, may result in differences in protein value and protein availability.

Principal Component Analysis and Cluster Analysis To Discriminate and Classify Protein Inherent Structure Chemical Makeup. *Cluster Analysis for Protein Intrinsic Structure.* Cluster analysis can be used to cluster IR spectra on the basis of their similarity with other spectra. In this study, Ward's algorithm method was used without any prior parametrization of the spectral data (original protein amide I FSD spectral data) in the IR region (ca. 1710–1576 cm^{-1}). This method helps to discriminate differences in structure chemical makeup between different tissues.

Figure 2 displays the results in the form of a dendrogram. From this diagram, two classes can be distinguished below a linkage distance less than 15, with Valier forming a separate group. Depending on the aggregation level (horizontal axis), different explanations can be inferred. The Valier group forms one distinct group just below an aggregation (linkage) distance 11. The Harrington group forms one distinct group below an aggregation (linkage) distance 15. They form a single group at an aggregation distance of about 16. In other words, Valier can be grouped together with the Harrington group for a linkage distance equal to about 16. **Figure 2** shows significantly different protein spectral clusters between Harrington and Valier barley,

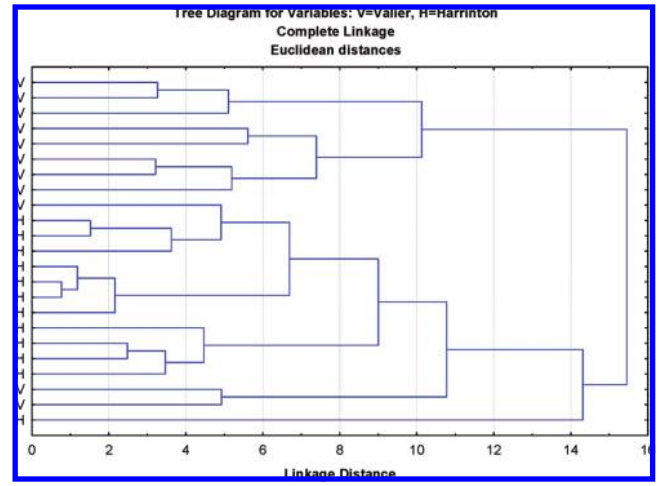

Figure 2. CLA cluster of synchrotron-based protein amide I FSD spectrum (1710–1576 cm^{-1}) obtained from Harrington (H) and Valier barley (V) at a cellular level (pixel size 10 μm × 10 μm) from all original spot spectrum [CLA analysis: (1) FSD spectral region, amide I, 1710–1576 cm^{-1}; (2) distance method, Euclidean; (3) cluster method, Ward's algorithm].

indicating that (1) the Valier and Harrington barley can be almost distinguished, and (2) their protein structural chemical makeup was different. Only two Valier protein spectra were convergent with those of Harrington (**Figure 2**); the others differed from those of Harrington.

Principal Component Analysis for Protein Intrinsic Structure. The second multivariate analysis tested was PCA analysis, a statistical data reduction method. In this barley protein inherent structure study, PCA analysis was used to identify the main sources of variation in the synchrotron-based protein amide I FSD spectra in the region 1710–1576 cm^{-1} of Harrington and Valier barley at a cellular level and identify features that differed between these two varieties of barley.

Figure 3show results from PCA analysis of the synchrotron FTIR spectrum data obtained from Valier and Harrington (V, H). First, three PCs (obtained after data reduction) were plotted (**Figure 3a**,**b**). These show that the PCA analysis could fully distinguish between the Valier and Harington in protein amide I FSD spectrum at the region of 1710–1576 cm^{-1}; Valier and Harrington can be grouped into separate ellipses (**Figure 3a**,**b**) with no overlap of groups. The first three PCs individually explain 36.1, 22.6, and 16.0% of the variation in the protein amide FSD spectrum data set.

Differences in Carbohydrate Molecular Structural Chemical Makeup. *Harrington versus Valier Barley.* The major absorption bands from carbohydrates are found in the 1180–950 cm^{-1} region of the infrared spectrum (*32*) and are attributed to C−O stretching vibrations. Bands in this region are complex (*33*). When studying plant materials, it is customary to search for structural carbohydrates such as hemicellulose and nonstructural carbohydrates such as starch (*2*). A peak area at ca.1420 cm^{-1} can be used to look for one particular type of carbohydrate, β-glucan (*2*). In the portion of the spectrum from 1550 to 800 cm^{-1}, strong carbohydrate bands are present for both structural and nonstructural carbohydrate, particularly in the region 1180–950 cm^{-1}. One major difference between these two forms of carbohydrate is the presence of bands of moderate intensity at approximately 1420, 1370, and 1335 cm^{-1}; these reflect characteristics of structural carbohydrates (*2, 7*). Carbohydrate band peaks between 1100 and 1025 cm^{-1} depend on whether the carbohydrate is structural or nonstructural. A peak

Table 5. Structural Characteristics of Carbohydrate (CHO) in the Endosperm in Terms of the Component Peak Height of Barley Seeds, Detected with Synchrotron-Based FTIR Microspectroscopy: Comparison of Harrington (Malting-Type) and Valier (Feed-Type) Barley CHO Component Peak Position

items	sample number	carbohydrate (CHO) component based on the CHO peak height[a] first peak (±SD[b])	second peak (±SD)	third peak (starch) (±SD)
barley varieties				
Harrington	26	0.3 (±0.2)	0.5 (±0.2)	0.8 (±0.3)
Valier	26	0.4 (±0.2)	0.6 (±0.3)	1.0 (±0.4)
SEM[c]		0.04	0.05	0.08
statistics (*P* value)				
feed		0.1059	0.0622	0.0709

[a] The carbohydrate data unit, IR absorbance unit. CHO peak baseline and region, 1180−800 and 1180 and 950 cm^{-1}, respectively. The barley CHO in the endosperm region has three major component peaks with the first, second, and third peaks at 1150, 1080, and 1025 cm^{-1}, respectively. [b] SD = standard deviation of mean. [c] SEM = pooled standard error of means; means with the same letter in the same column are not significantly different ($P > 0.05$) by Fisher's protected LSD method.

Table 6. Structural Characteristics of Carbohydrate (CHO) in the Endosperm in Terms of the CHO Component Peak Height Ratios of Barley Seeds, Detected with Synchrotron-Based FTIR Microspectroscopy: Comparison of Harrington (malting-type) and Valier (feed-type) Barley

items	sample number	carbohydrate (CHO) component ratios based on the CHO peak height[a] ratio of CHO peak 1 to 2 (±SD[b])	ratio of CHO peak 1 to 3 (±SD)	ratio of CHO peak 2 to 3 (±SD)
barley varieties				
Harrington	26	0.6 (±0.1)	0.4 (±0.1)	0.6 (±0.04)
Valier	26	0.6 (±0.1)	0.4 (±0.1)	0.7 (±0.1)
SEM[c]		0.01	0.010	0.012
statistics (*P* value)				
feed		0.7726	0.9163	0.8438

[a] The carbohydrate data unit, IR absorbance unit. CHO peak baseline and region, 1180−800 and 1180 and 950 cm^{-1}, respectively. The barley CHO in the endosperm region has three major component peaks with the first, second, and third peaks at 1150, 1080, and 1025 cm^{-1}, respectively. [b] SD = standard deviation of mean. [c] SEM = pooled standard error of means; means with the same letter in the same column are not significantly different ($P > 0.05$) by Fisher's protected LSD method.

at ca. 1025 cm^{-1} indicates nonstructural carbohydrate such as starch in the endosperm of cereal grain (*2, 7*). A peak at ca. 1240 cm^{-1}indicates a structural carbohydrate such as hemicellulose. The carbohydrate structural makeup study was focused on the barley endosperm region in which the carbohydrates are primarily nonstructural with three major infrared components centered at 1150, 1080, and 1025 cm^{-1} (*33, 34*)

Table 5 shows the structural characteristics of carbohydrate (CHO) in the endosperm in terms of the carbohydrate component peak profile of barley seeds detected with the synchrotron-based analytical technique. No significant differences in carbohydrate component peak profiles were detected for Harrington and Valier barley with averages of 0.36, 56, and 0.88 absorbance unit ($P > 0.05$) for the peaks at 1150, 1080, and 1025 cm^{-1}, respectively. This indicates that the carbohydrate component profile was similar between these two barley varieties. **Table 6** shows the structural characteristics of carbohydrate (CHO) in the endosperm in terms of the peak ratios of the CHO

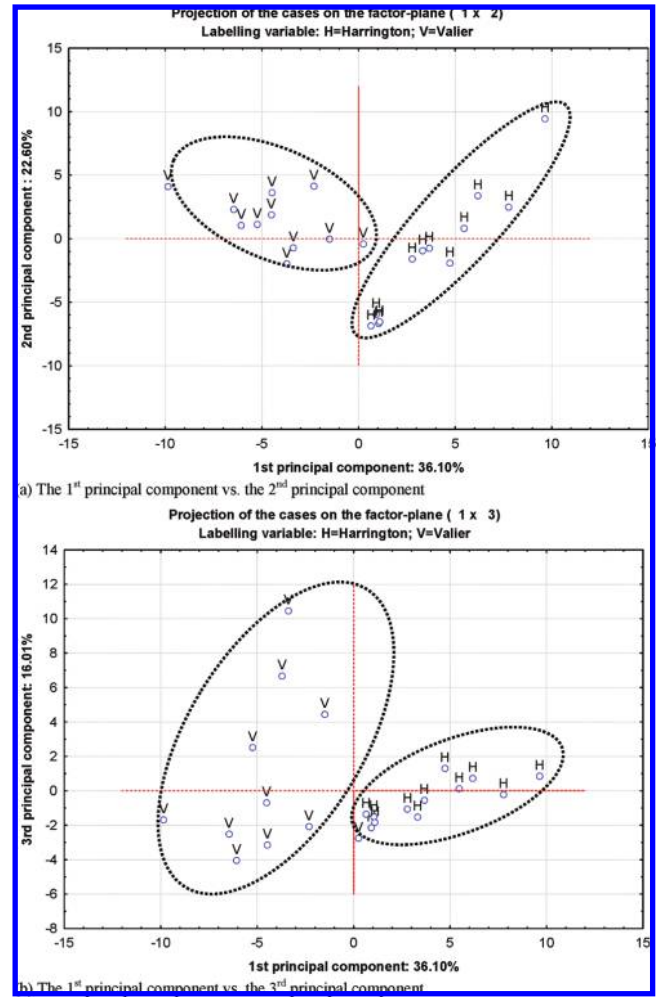

Figure 3. Scatter plot of the first principal component vs the second principal component (**a**) and the third principal component (**b**) of PCA analysis of synchrotron-based protein FSD protein amide I spectrum (1710−1576 cm^{-1}) obtained from Harrington and Valier barley at a cellular level (pixel size 10 μm × 10 μm) from all original spot spectrum: The firsth, second, and third principal component explains 36.1, 22.6 and 16.01% of the total variance, respectively.

component of barley seeds. No significant differences between the two barleys in carbohydrate component peak ratios were detected, indicating similarity between the two barley varieties.

Principal Component Analysis and Cluster Analysis Unable To Discriminate and Classify Carbohydrate Structures between Harrington and Valier Barley. *Cluster Analysis for Carbohydrate Intrinsic Structure.* In this study, Ward's algorithm method was used without prior parametrization of the spectral data (used original carbohydrate spectral data) in the 1180–800 cm^{-1} region. **Figure 4** displays the results in the form of a dendrogram. From this diagram, the two varieties of barley cannot be fully distinguished regarding inherent carbohydrate structures; they were similar.

Principal Component Analysis for Carbohydrate Intrinsic Structure. PCA analysis was used to identify the main sources of variation in the synchrotron-based carbohydrate spectra in the region 1180–800 cm^{-1} of Harrington and Valier barley at a cellular level and identify features that differed between the two varieties of barley. **Figure 5** shows results from PCA analysis of the synchrotron FTIR spectrum data obtained from Valier and Harrington (V, H). The first three PCs (obtained after data reduction) were plotted (**Figure 5a**,**b**), showing that the

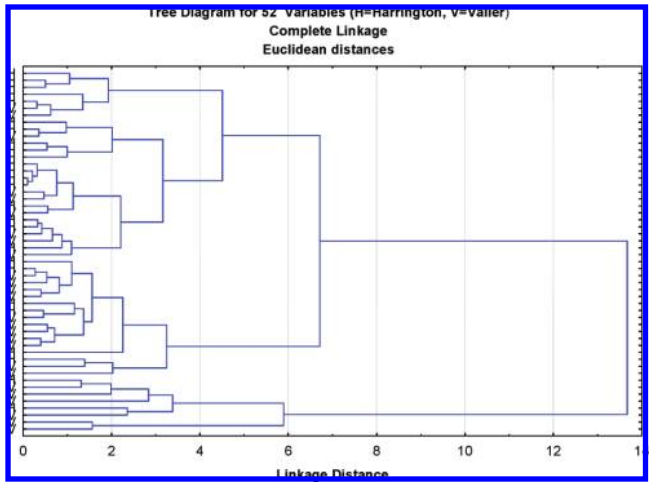

Figure 4. CLA cluster of synchrotron-based carbohydrate spectrum (1180–800 cm^{-1}) obtained from Harrington (H) and Valier barley (V) at a cellular level (pixel size 10 μm × 10 μm) [CLA analysis: (1) carbohydrate spectral region, amide I, 1180–800 cm^{-1}; (2) distance method, Euclidean; (3) cluster method, Ward's algorithm].

PCA analysis could not fully distinguish between the Valier and Harrington in terms of the carbohydrate structure spectrum and therefore Valier and Harrington could not be grouped in separate ellipses (**Figure 5a**,**b**) without overlapping of groups. The first three PCs individually and sequentially explain 85.3, 8.1, and 4.6% of the variation in the carbohydrate structure spectrum data set. These results indicate that the carbohydrate molecular chemical makeup and inherent structure were similar or not detectable between these two barley varieties.

Further Discussion on Protein and Carbohydrate Molecular Chemical-Structural Makeup of Barley. In the preliminary study, we used the SFTIRM to measure the starch to protein ratio in the microstructural matrix of endosperm tissue between the two barleys and tried to detect a cause for the different degradation characteristics between these two barley varieties. The hypothesis in that study was that the different degradation characteristics between the two barley varieties was due to differences in the starch−protein matrix of the endosperm tissue. These results showed a wider range in the starch to protein IR absorbance intensity ratio for Harrington than Valier, suggesting that the ratio is more heterogeneous in the endosperm chemical makeup for Harrington. Valier had a lower ratio of starch to protein IR absorbance intensity than Harrington (4.12 vs 2.78). This implies that the starch granules in Valier are more closely associated with the protein matrix. This closer association may prevent the starch granules from being degraded rapidly in the rumen.

To confirm the above finding, we conducted a confirmation study. These results showed that Harrington and Valier barley did not differ in the starch to protein IR absorbance intensity ratio, despite the trend that was similar to the previous study with a slightly lower ratio starch to protein in endosperm tissues of Valier.

These different results from these two separate studies made us reconsider the cause for the different degradation behavior between Harrington and Valier barley. Association of the protein matrix with the starch granules in the endosperm tissue may not be sole cause. Therefore, we examined the differences in protein and carbohydrate molecular structural chemical makeup in terms of (1) structural differences in protein amide I to amide II ratio, (2) structural differences in protein secondary structure

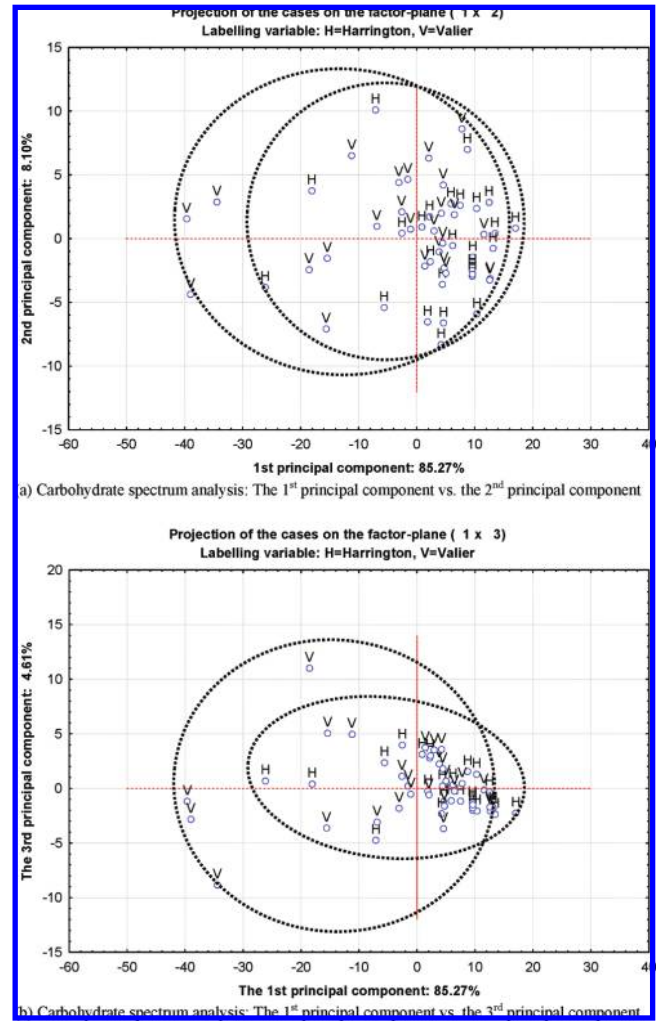

Figure 5. Scatter plot of the first principal component vs the second principal component (**a**) and the third principal component (**b**) of PCA analysis of synchrotron-based carbohydrate spectrum (1180−800 cm^{-1}) obtained from Harrington and Valier barley at a cellular level (pixel size 10 μm × 10 μm): The first, second, and third principal component explains 85.3, 8.1, and 4.6% of the total variance, respectively.

profile, and (3) structural differences in carbohydrate component peak profile within the seed tissues.

From our results, we concluded that although Harrington and Valier are similar in chemical composition, they differ significantly in their protein amide I and amide II intensities as well as the amide I to amide II ratios (**Table 2**). Furthermore, they differ significantly in their protein secondary structure profile, the relative percentage of secondary structures, and the secondary ratio (**Tables 3** and **4**). Harrington was lower than Valier in amide I and amide II and in the ratio of amide I to amide II and higher in protein α-helix and β-sheet but lower in the other proteins (β-turn and random coil). These results clearly indicate that protein molecular structural chemical makeup or protein conformation was significantly different between the two barleys. Cluster analysis (**Figure 2**) and PCA (**Figure 3**) analysis confirmed this finding.

Harrington and Valier were not detectably different in carbohydrate molecular structural chemical makeup (**Tables 5** and **6**). Again CLA and PCA analysis detected no difference in carbohydrate structure (**Figures 4** and **5**) between these two barley varieties. Because no previous publications were found in this area, no comparison could be made. Our results imply that differences in the protein molecular structural chemical

makeup may play an important role in causing the different degradation behavior between the two barley varieties, not carbohydrate makeup. Advanced synchrotron-based technology was the basis for this concept based on molecular structure research. Advanced synchrotron technology (SFTIRM) should prove useful to enhance our knowledge of molecular structural chemical research of plants, feed, and seeds.

In conclusion, on the basis of the synchrotron-based analytical technique, the protein and carbohydrate molecular structural chemical makeup of barleys could be revealed. Components were identified in the endosperm at a high ultraspatial resolution within cellular dimensions. Differences between the two barley varieties in protein molecular structural chemical makeup were identified but no difference in carbohydrate molecular structural chemical makeup were detected. Harrington barley had less amide I and amide II and a lower ratio of amide I to amide II than Valier barley, a relatively higher percentage of model fitted α-helix and β-sheet, and less of other protein (β-turn and random coil). Our results demonstrate the potential of using a synchrotron-based analytical technique to reveal differences in molecular structural chemical makeup between feeds, seeds, and varieties. Further study is needed to quantify the relationship and fully understand differences between the molecular structural chemical makeup of barley varieties and correlate these findings with the nutritive value and digestive or fermentation behavior of various varieties of feeds and seeds.

ACKNOWLEDGMENT

We are grateful to B. Rossnagel (University of Saskatchewan) for providing seed samples, J. McKinnon, C. Christensen, and D. Christensen for general research support, and Jennifer Bohon, Nebojsa Marinkovic, Lisa Miller, Wang Qi, and Alexander Ignatov (NSLS-BNL, U.S. Department of Energy, New York) for helpful data collection at U10B and U2B experimental stations.

LITERATURE CITED

(1) Budevska, B. O. In *Handbook of Vibrational Spectroscopy, Vol. 5. Applications of Vibrational Spectroscopy in Life, Pharmaceutical and Natural Sciences*; Chalmers, J. M., Griffiths, P. R., Eds.; John Wiley and Sons, Inc.: New York, 2002; pp 3720−3732.

(2) Wetzel, D. L.; Eilert, A. J; Pietrzak, L. N; Miller, S. S.; Sweat, J. A. Ultraspatially-resolved synchrotron infrared microspectroscopy of plant tissue in situ. *Cell. Mol. Biol.* **1998**, *44*, 145–167.

(3) Diem, M.; Boydston-White, S.; Chiriboga, L. Infrared spectroscopy of cells and tissues: Shining light onto a novel subject. *Appl. Spectrosc.* **1999**, *53*, 148–161.

(4) Miller, L. M. Infrared microspectroscopy and imaging. Available at http://nslsweb.nsls.bnl.gov/nsls/pubs/nslspubs/imaging0502/irxrayworkshopintroduction.ht . Accessed October 1, 2002.

(5) Marinkovic, N. S.; Huang, R.; Bromberg, P.; Sullivan, M; Toomey, J.; Miller, L. M.; Sperber, E.; Moshe, S.; Jones, K. W.; Chouparova, E.; Lappi, S.; Franze, S.; Chance., M. R. Center for Synchrotron Biosciences' U2B beamline: An international resource for biological infrared spectroscopy. *J. Synchrotron Radiat.* **2002**, *9*, 189–197.

(6) Yu, P. Synchrotron IR microspectroscopy for protein structure analysis: Potential and questions: A review. *Spectroscopy* **2006**, *20*, 229–251. (Invited Review Article).

(7) Wetzel, D. L. When molecular causes of wheat quality are known, molecular methods will supercede traditional methods. *Proceedings of the International Wheat Quality Conference II, Manhattan, Kansas, May 2001*; 2001; pp 1–20.

(8) Miller, L. M.; Carr, G.; Jackson, M.; Williams, Y.; Dumas, P. The impact of infrared synchrotron radiation on biology: Past, present, and future. *Synchrotron Radiat. News* **2000**, *13*, 31–37.

(9) Yu, P.; Christensen, D. A.; Christensen, C. R.; Drew, M. D.; Rossnagel, B. G.; McKinnon, J. J. Use of synchrotron FTIR microspectroscopy to identify chemical differences in barley endosperm tissue in relation to rumen degradation characteristics. *Can. J. Anim. Sci.* **2004**, *84*, 523–527.

(10) Kemp, W. *Organic Spectroscopy*, 3rd ed.;W.H. Freeman and Co.: New York, 1991.

(11) Himmelsbach, D. S.; Khalili, S.; Akin., D. E. FT-IR microspectroscopic imaging of flax (*Linum usitatissimum* L.) stems. *Cell. Mol. Biol.* **1998**, *44*, 99–108.

(12) Jackson, M.; Mantsch, H. H. Ex vivo tissue analysis by infrared spectroscopy. In *Encyclopedia of Analytical Chemistry*; Meyers, R. A., Ed.; John Wiely & Sons: New York, 2000; Vol. 1, 131–156..

(13) Yu, P. Multicomponent peak modeling of protein secondary structures: Comparison of Gaussian with Lorentzian analytical methods for plant feed and seed molecular biology and chemistry research. *Appl. Spectrosc.* **2005**, *59*, 1372–1380.

(14) Kauppinen, J. K.; Moffatt, D. J.; Mantsch, H. H.; Cameron., D. G. Fourier self-deconvolution: A method for resolving intrinsically overlapped bands. *Appl. Spectrosc.* **1981**, *35*, 271–276.

(15) Griffths, P. R.; Pariente, G. Introduction to spectral deconvolution. *Trends Anal. Chem.* **1986**, *5*, 209–215.

(16) Ørskov, E. R.; McDonald., I. The estimation of protein degradability in the rumen from incubation measurements weighted according to the rate of passage. *J. Agric. Sci. (Cambridge)* **1979**, *92*, 499–503.

(17) Tamminga, S.; Van Straalen, W. M.; Subnel, A. P. J.; Meijer, R. G. M.; Steg, A.; Wever, C; Blok., M. C. The Dutch protein evaluation system: The DVE/OEB-system. *Livestock Prod. Sci.* **1994**, *40*, 139–155.

(18) SAS. *User's Guide: Statistics*, 8th ed.; SAS Inst., Inc.: Cary, NC, 2003.

(19) Cytospec, Software for infrared spectral imaging, Version 1.1.01; 2004.

(20) Sockalingum, G. D.; Bouhedja, W. P; Pina, P; Allouch; Bloy, C.; Manfait., M. FT-IT spectroscopy as an emerging method for rapid characterization of microorganisms. *Cell. Mol. Biol.* **1998**, *44*, 261–269.

(21) Nocek, J. E.; Tamminga., S. Site of digestion of starch in the gastrointestinal tract of dairy cows and its effect on milk yield and composition. *J. Dairy Sci.* **1991**, *74*, 3598–3629.

(22) Givens, D. I.; Clark, P.; Jacklin, D.; Moss, A. R.; Savery, C. R. Nutritional aspect of cereal, cereal grain by-products and cereal straw for ruminants. *Home-Grown Cereals Authority, Research Review*. Hamlyn House, Highgate Hill, London, England, 1993; Vol. 24, 1–180.

(23) Gibson, L. A.; Bowman, J. G. P.; Oberthur, L. E.; Blake, T. K. Determination of genetic markers associated with ruminant digestion of barley. *Proceedings, Western Section, American Society of Animal Science*; 1994; Vol. 45, 108–110.

(24) Bowmanzpt, J. G. P.; Blake, T. K.; Surber, L. M. M.; Habernicht, D. K.; Daniels, T. K.; Daniels, J. T. Genetic factors controlling digestibility of barley for ruminants. *Proceedings Western Section, American Society of Animal Science*; retrieved in June 2001.

(25) Yu, P. Application of advanced synchrotron radiation-based Fourier transform infrared (SR-FTIR) microspectroscopy to animal nutrition and feed science: A novel approach. *Br. J. Nutr.* **2004**, *92*, 869–885.

(26) NRC. *Nutrient Requirement of Beef cattle (7th ed). National Research Council*; National Academy Press: Washington, DC, 1996.

(27) NRC. *Nutrient Requirement of Dairy Cattle (7th ed). National Research Council*; National Academy Press: Washington, DC, 2001.

(28) Kneipp, J.; Miller, L. M.; Joncic, M; Kittel, M; Lasch, P.; Beekes, M; Naumann., D. In situ identification of protein structural changes in prion-infected tissue. *Biochim. Biophys. Acta* **2003**, *1639*, 152–158.

(29) Wang, Q.; Kretlow, A.; Beekes, M.; Naumann, D.; Miller, L. In situ characterization of prion protein structure and metal accumulation in scrapie-infected cells by synchrotron infrared and X-ray imaging. *Vib. Spectrosc.* **2005**, *38*, 61–69.
(30) Martin, M. C. Fourier-transform infrared spectroscopy. Available at http://infrared.als.lbl.gov/. Accessed October 1, 2002.
(31) Wetzel, D. L.; Srivarin, P.; Finney, J. R. Revealing protein infrared spectral detail in a heterogeneous matrix dominated by starch. *Vib. Spectrosc.* **2003**, *31*, 109–114.
(32) Mathlouthi, M.; Koenig., J. L. Vibrational spectra of carbohydrates. *Adv. Carbohydr. Chem. Biochem.* **1986**, *44*, 7-–89.
(33) Yu, P.; McKinnon, J. J.; Christensen, C. R.; Christensen, D. A. Imaging molecular chemistry of pioneer corn. *J. Agric. Food Chem.* **2004b**, *52*, 7345–7352.
(34) Yu, P; Block, H.; Ni, Z.; Doiron, K. Rapid characterization of molecular chemistry, nutrient make-up and microlocation of internal seed tissue. *J. Synchrotron Radiat.* **2007**, *14* 382–390.

Received for review October 29, 2007. Revised manuscript received February 23, 2008. Accepted February 25, 2008. This research has been supported by grants from Natural Sciences and Engineering Research Council of Canada (NSERC- Individual Discovery Grant). The National Synchrotron Light Source in Brookhaven National Laboratory (NSLS-BNL, New York) is supported by the U.S. Department of Energy Contract DE-AC02-98CH10886. The Center for Synchrotron Biosciences, Center for Proteomics, Case Western Reserve University, is supported by the National Institute for Biomedical Imaging and Bioengineering under P41-EB-01979.

JF800015X